

This article can be cited before page numbers have been issued, to do this please use: P. M. Sonar, S. P. Singh, E. L. Williams, S. Manzhous and A. Dodabalapur, *Phys. Chem. Chem. Phys.*, 2013, DOI: 10.1039/C3CP52929K.



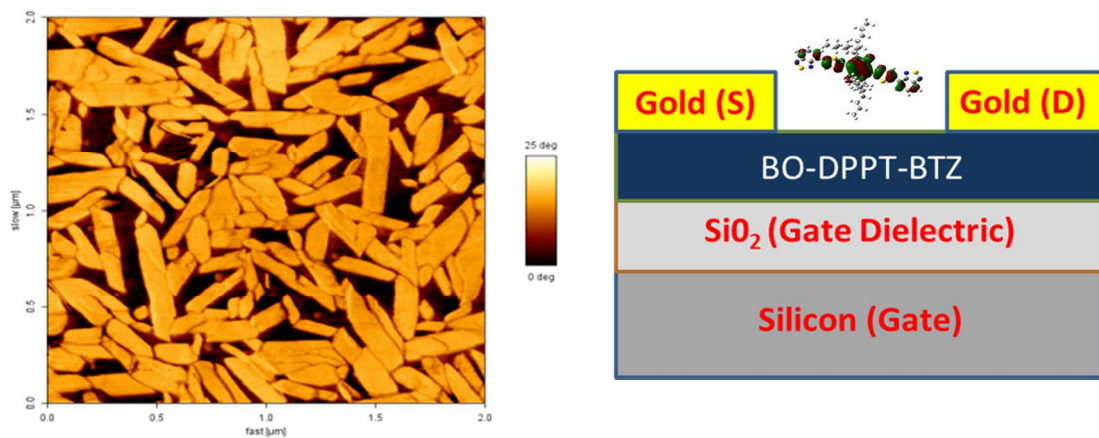
This is an *Accepted Manuscript*, which has been through the RSC Publishing peer review process and has been accepted for publication.

Accepted Manuscripts are published online shortly after acceptance, which is prior to technical editing, formatting and proof reading. This free service from RSC Publishing allows authors to make their results available to the community, in citable form, before publication of the edited article. This *Accepted Manuscript* will be replaced by the edited and formatted *Advance Article* as soon as this is available.

To cite this manuscript please use its permanent Digital Object Identifier (DOI®), which is identical for all formats of publication.

More information about *Accepted Manuscripts* can be found in the [Information for Authors](#).

Please note that technical editing may introduce minor changes to the text and/or graphics contained in the manuscript submitted by the author(s) which may alter content, and that the standard [Terms & Conditions](#) and the [ethical guidelines](#) that apply to the journal are still applicable. In no event shall the RSC be held responsible for any errors or omissions in these *Accepted Manuscript* manuscripts or any consequences arising from the use of any information contained in them.



A benzothiadiazole end-capped donor-acceptor-donor (D-A-D) based small molecule BO-DPP-BTZ has been synthesized. BO-DPP-BTZ as an active layer exhibited a hole mobility of $0.06 \text{ cm}^2/\text{Vs}$ in OFETs.

Cite this: DOI: 10.1039/c0xx00000x

www.rsc.org/xxxxxx

ARTICLE TYPE

Benzothiadiazole End Capped Donor-Acceptor Based Small Molecule for Organic Electronics

Prashant Sonar,^{a,*} Evan L. Williams^a, Samarendra P. Singh^{a,b}, Sergei Manzhos,^c
Ananth Dodabalapur^{a, d,*}

Received (in XXX, XXX) Xth XXXXXXXXX 20XX, Accepted Xth XXXXXXXXX 20XX

DOI: 10.1039/b000000x

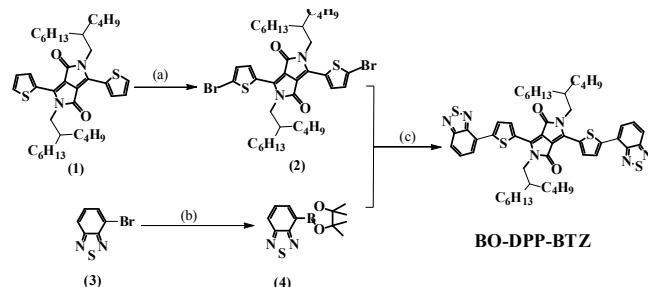
A benzothiadiazole end-capped small molecule 3,6-bis(5-(benzo[c][1,2,5]thiadiazol-4-yl)thiophen-2-yl)-2,5-bis(2-butylloctyl)pyrrolo[3,4-c]pyrrole-1,4(2H,5H)-dione (BO-DPP-BTZ) using a fused aromatic moiety DPP (at the centre) is designed and synthesized. BO-DPP-BTZ is a donor-acceptor-donor (D-A-D) structure which posses a band gap 1.6 eV and exhibit a strong solid state ordering inferred from ~120 nm red shift of the absorption maxima from solution to thin film. Field-effect transistors utilizing a spin coated thin film of BO-DPP-BTZ as an active layer exhibited a hole mobility of 0.06 cm²/Vs. Solution-processed bulk heterojunction organic photovoltaics employing a blend of BO-DPP-BTZ and [70]PCBM demonstrated a power conversion efficiency of 0.9%.

Over the last few years, the research interest in diketopyrrolopyrrole (DPP) based organic semiconductors for applications in organic electronics has grown rapidly with reports of high performances organic field-effect transistors (OFETs) and organic photovoltaic (OPV) devices.¹ DPP is a fused aromatic planar conjugated block with two electron withdrawing carbonyl groups and lactam nitrogen for alkyl functionalization.² There exist numerous published reports on thiophene-flanked DPP, D-A-D based high performance polymers.³ Considerably less attention has been focused on the development of monodispersed high performance small molecules which may provide benefits in comparison to polymers in terms of batch to batch reproducibility and high purity.⁴ To the best of our knowledge, the first DPP functionalized oligothiophene was reported by Nguyen *et al.*, and small molecule, solution-processed BHJ solar cells showed a reasonably good power conversion efficiency (PCE).⁵ Similar organic materials with different alkyl groups were designed, synthesized and used successfully by the same group. OFET devices employing a solution processed thin film showed a hole mobility of 0.02 cm²/Vs.⁶ Our group reported DPP-based materials using trifluoromethyl phenyl or di/tri fluoro phenylene end capping groups attached to the DPP as the first successful acceptor materials in OPV applications; the highest performance of 1% was achieved using P3HT as a donor material in a BHJ architecture.⁷ By using benzofuran units attached to the DPP, another solution processable highly efficient donor was developed and used in OPV devices by Nguyen *et al.* Impressive

performance of 4.4% PCE in BHJ devices was achieved using this small molecule.⁸ Recently, Wurthner *et. al.* reported dicyano-substituted DPP with shorter branched alkyl side chain for OFETs and the highest hole mobility of 0.7 cm²/Vs was measured using vacuum deposited thin films of this.⁹ Luscombe *et. al* studied the BHJ device properties of the oligoselenophene derivatives of DPP (analogous to the DPP-oligothiophene structures) and the highest PCE of 1.53 % was measured. Upon testing these materials in OFETs, the highest hole mobility of 4x10⁻⁵ cm²/Vs was reported.¹⁰ An amphiphilic π -conjugated low energy gap small molecule with terminal lipophilic paraffinic chains and lateral hydrophilic triglyme chain oligomer was reported by Reynolds *et al.*¹¹ The highest hole mobility of 3.4 x10⁻³ cm²/Vs and PCE of 0.68 % was reported for this material. A naphthodithiophene symmetrically substituted to DPP unit was reported by Marks *et al.*¹² This donor molecule was used in both OPV and OFET devices, the highest reported values for PCE and hole mobility were 4.06 % and a of 7.18 x 10⁻³ cm²/Vs, respectively. Fréchet *et al.* used the planar and symmetric end-group strategy to direct the molecular self-assembly of DPP small molecules. The highest PCE of 4.1 % was achieved in BHJ devices.¹³ Very recently, a three dimensional star-shaped small molecule with a triphenylamine core and diketopyrrolopyrrole arm was reported. Interestingly, this molecule works as an acceptor¹⁴ as well as donor¹⁵ in OPV devices. Using it as an acceptor, a PCE of 1.20% was reported (with P3HT) whereas using it as a donor it gives PCE of 1.81% (with PCBM). An alkyne-functionalized DPP donor material was reported by Mark *et al.*¹⁶ Good hole mobility values of 0.17 cm²/Vs in OFETs and a PCE of 2% in OPV devices were reported for this molecule. A dicyanomethylene-substituted quinoidal DPP was prepared by Zhu *et al.*¹⁷ Both solution and vacuum deposited thin film OFETs exhibited an electron mobility of 0.35 cm²/Vs. Among all these, there are very few small molecules which exhibit high performance in solution processed OFET devices.

In this paper, we report the design and a synthesis of a novel solution processable benzothiadiazole end capped DPP acceptor-donor-acceptor-donor-acceptor (A-D-A-D-A) based organic semiconductor (Scheme 1). The benzothiadiazole and the central DPP core act as an acceptor whereas the thiophene acts as a donor. This small molecule has proved to be a promising material for high mobility solution processable OFETs. The intention behind the design of this small molecular structure is to enhance the degree of coplanarity by attaching another fused benzothiadiazole ring at the end of DPP. Such fused ring

structures can generate strong intramolecular interactions and π - π stacking via the sulfur-nitrogen interaction and a large molecular orbital overlapping area.¹⁸ Additionally, due to the attachment of the benzothiadiazole moiety at the end of thiophene-DPP-thiophene, D-A-D interactions may improve further and result in more effective charge transport.



Scheme 1 Reagents and conditions: (a) Bromine, chloroform, room temp., overnight, 78%; (b) Bis(pinacolato)diboron, potassium acetate, PdCl₂(dppf), 1,4-dioxane, 80°C for 20h, 62%; (c) Pd(PPh₃)₄, aliquat 336, 2M K₂CO₃, toluene, 80°C for 72h, 87%.

First, the core 2,5-bis(2-butylloctyl)-3,6-di(thiophen-2-yl)pyrrolo[3,4-c]pyrrole-1,4(2H,5H)-dione (**1**) can be easily synthesized by using respective heteroaryl carbonitriles followed by alkylation according to a previously reported procedure.¹³ The branched alkyl chain butyl-octyl was selected to improve solubility. Compound **1** was brominated using bromine in chloroform at room temperature, which yielded dibromo derivative 3,6-bis(5-bromothiophen-2-yl)-2,5-bis(2-butylloctyl)pyrrolo[3,4-c]pyrrole-1,4(2H,5H)-dione (**2**). Compound 4-bromobenzo[c][1,2,5]thiadiazole (**3**) was synthesized according to a previously reported procedure.¹⁹ Compound **3** was then converted to the 4-(4,4,5,5-tetramethyl-1,3,2-dioxaborolan-2-yl)benzo[c][1,2,5]thiadiazole (**4**) using bis(pinacolato)diboron, PdCl₂(dppf) and KOAc in 1,4-dioxane. Standard Suzuki coupling of compounds **2** and **4** gave the final compound 3,6-bis(5-(benzo[c][1,2,5]thiadiazol-4-yl)thiophen-2-yl)-2,5-bis(2-butylloctyl)pyrrolo[3,4-c]pyrrole-1,4(2H,5H)-dione (**BO-DPP-BTZ**). **BO-DPP-BTZ** was purified by column chromatography using hexane:chloroform solvent mixture and then the final compound was obtained with a 58% yield.

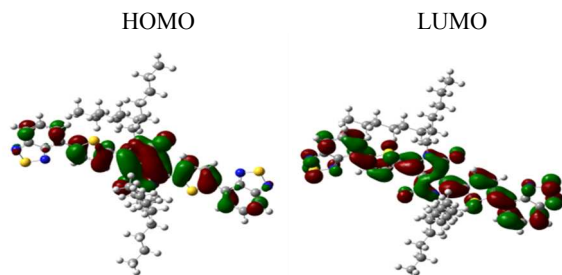


Figure 1. The optimized geometries and electron density isocontours of the HOMO and LUMO orbitals of **BO-DPP-BTZ** (Atom color code: yellow-sulfur, blue-nitrogen, dark grey-carbon, light grey-hydrogen. Green and brown-are used for different signs of the wave functions).

Density functional theory (DFT) calculations were performed on **BO-DPP-BTZ** to identify the electron density distribution of the

frontier orbitals. The B3LYP functional²⁰ and 6-31g(d,p) basis were used. The chloroform solvent was modeled with the Polarized Continuum Model (PCM).²¹ The UV-vis absorption spectrum was computed using the CAM-B3LYP functional to account for the charge transfer character of the transitions.²² The calculations were performed in Gaussian 09.²³ The optimized geometries and electron density isocontours of the highest occupied molecular orbital (HOMO) and lowest unoccupied molecular orbital (LUMO) of **BO-DPP-BTZ** are shown in Figure 1. The HOMO appears primarily localized on the DPP moiety but is distributed throughout the molecule. The LUMO appears distributed throughout the molecule with a greater density of the benzothiadiazole than the HOMO. The theoretically predicted HOMO and LUMO energy values are 5.04 eV and 3.06 eV, respectively. The theoretical band gap calculated from these energy level differences is 1.985 eV.

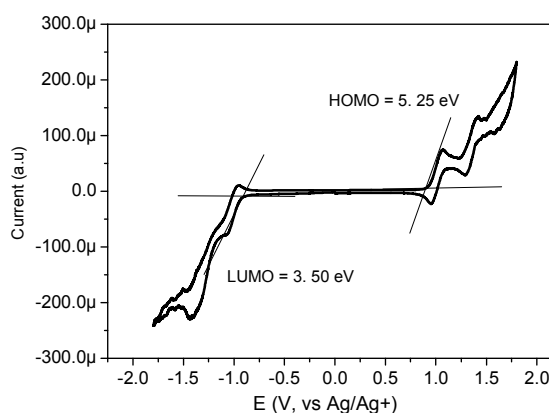
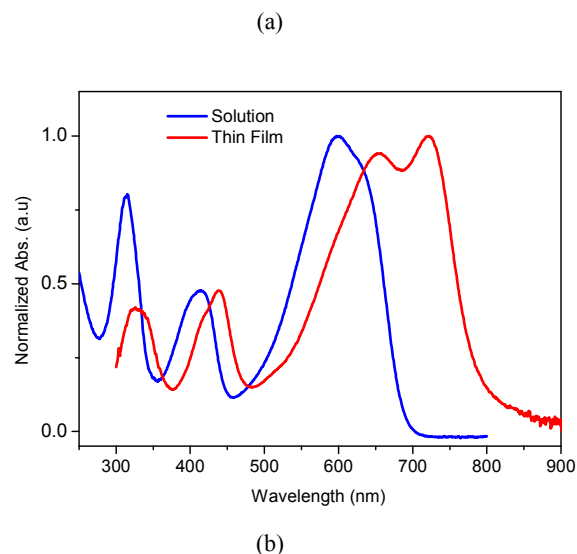


Fig. 2 (a) UV-vis absorption spectra of **BO-DPP-BTZ** in chloroform solution and thin film, spin coated from chloroform solution; (b) cyclic voltammogram of **BO-DPP-BTZ** at a scan rate 100 mVs⁻¹. The electrolyte was 0.1 M TBAPF₆/anhydrous dichloromethane.

The thermal properties of **BO-DPP-BTZ** were investigated by the thermogravimetric analysis (TGA) and differential scanning calorimetry (DSC) techniques. TGA showed a 5% weight loss (decomposition temperature) at 410.47 °C under nitrogen, representing high thermal stability. During the heating and

cooling cycle of the DSC measurement, endothermic and exothermic peaks were observed at 182 °C and 149 °C, respectively. These peaks are attributed to the melting and crystallization temperatures of this small molecule (see Supplementary Information). The solution and thin film optical properties of **BO-DPP-BTZ** were studied by UV-vis absorption spectroscopy. For solution measurements, **BO-DPP-BTZ** was dissolved in chloroform; for solid state measurement, a thin film of **BO-DPP-BTZ** was spin coated from a chloroform solution onto a glass slide. In both case the spectra have multiple absorption peaks due to the various constituent donor and acceptor building blocks in the conjugated backbone, and their subsequent interaction. This is a typical and commonly seen feature of D-A conjugated systems.²⁴ The absorption maximum (λ_{max}) measured in solution is at 598 nm whereas the maximum recorded in the solid state is at 722 nm. The computed main absorption peak maximum of 579 nm (see supporting information) is in excellent agreement with the experiment (see Fig. 2(a)). The roughly 120 nm red shift from solution to solid state is indicative of significant molecular organization and increased intermolecular interaction between molecules. The optical band gap calculated from the solution absorption cutoff is around 1.77 eV whereas from thin film cutoff is around 1.55 eV.

The electrochemical properties of **BO-DPP-BTZ** were investigated by cyclic voltammetry (CV). All CV measurements were done at room temperature with a conventional three electrode configuration consisting of a platinum wire working electrode, a gold counter electrode, and an Ag/AgCl reference electrode under argon using tetrabutylammonium hexafluorophosphate as an electrolyte at a scan rate of 100 mV/s in anhydrous dichloromethane. As shown in Figure 2, **BO-DPP-BTZ** exhibited reversible cathodic and anodic redox waves. The HOMO and LUMO energy levels were calculated from the oxidation and reduction onset potentials. These onset potentials were used for calculating ionization potential (IP) and electron affinity (EA) values based on -4.4 eV as the SCE energy level relative to vacuum ($EA = E_{\text{red-onset}} + 4.4$ eV, $IP = E_{\text{ox-onset}} + 4.4$ eV) (see Figure 2). Thus the HOMO and LUMO values for **BO-DPP-BTZ** are taken to be 5.25 eV and 3.50 eV respectively. We also measured the HOMO value of **BO-DPP-BTZ** with photoelectron spectroscopy in air (PESA), and the value of 5.35 eV was found to be in good agreement with CV data (see the PESA graph in supporting information). The electrochemical band gap calculated for **BO-DPP-BTZ** is 1.75 eV. The band gap and energy level values are found to be in a good agreement with the theoretical calculated values.

BO-DPP-BTZ was used as the active layer in top contact, bottom gate OFET devices. A 200 nm SiO₂ gate dielectric was deposited on a heavily n-doped conductive silicon wafer substrate for use in OFET devices. The active thin film of small molecule (~40 nm) was spin coated using 8 mg/ml solution in chloroform on top of an octyltrichlorosilane (OTS) modified SiO₂/Si surface. Gold source and drain electrodes were deposited on top of the **BO-DPP-BTZ** active layer via vacuum deposition. For a typical OFET device reported here, the S-D channel length (L) and channel width (W) were 100 μm and 1 mm, respectively. The FET measurements were done at room temperature under a dry nitrogen atmosphere using a Keithley 4200 parameter analyzer. The output and transfer characteristics of OFETs using **BO-DPP-BTZ** channel semiconductor are shown in Figure 3. The charge carrier mobilities were calculated from the saturation

regime of the OFET transfer characteristics using the following equation:

$$I_{\text{SD}} = C_i \mu_{\text{sat}} (W/2L) (V_G - V_T)^2$$

where I_{SD} is the drain current, W and L are, respectively, the semiconductor channel width and length, C_i is the capacitance per unit area of the gate dielectric, and V_G and V_T are, respectively, the gate voltage and threshold voltage. V_T of the device was determined from extrapolation of the linear fit of the ($I_{\text{SD}}/2$) vs V_G curve in the saturation regime at $I_D = 0$.

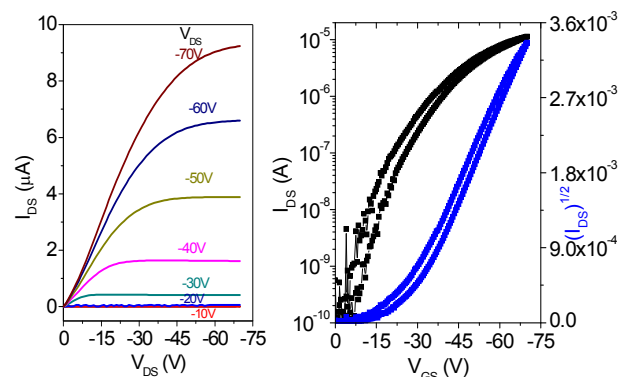


Fig. 3 Output (left) and transfer (right) characteristics of **BO-DPP-BTZ** OFET devices processed at room temperature. Device dimensions: channel length = 100 μm ; channel width = 1 mm. All devices were measured in a dry N₂ filled glove box.

The devices exhibit p-channel performance with the highest mobility of 0.06 cm²/V-sec. and a threshold voltage of -23 Volts. The current on/off ratio was calculated to be in the range of 10⁴-10⁵. Two cycles of forward and reverse bias, shown in the transfer characteristics, indicate a low hysteresis of $\Delta V_{\text{TH}} = 3$ Volts which indicates low charge carrier trapping in the OFET device. The mobility reported here is one of the higher values for a device using a small molecule synthesized in an elegant manner and fabricated using a solution-based processing method.^{4a} In comparison to the mobility of small molecule based oligothiophene derivatives bearing a diketopyrrolopyrrole core, such as DHT6DPPC6 and DHT6DPPC12 (0.02 and 0.01 cm²/V s), the mobility of **BO-DPP-BTZ** is three times higher.⁶ This enhancement in the mobility may be due to the incorporation of the electron withdrawing benzothiadiazole group at the end of DPP which enhances the D-A and S-N interactions.^{18,24} There is also a report on DPP core based OFETs which gives a hole mobility of 0.013 cm²/V s in solution processed devices.²⁵ Both these examples (with structures analogous to **BO-DPP-BTZ**) clearly indicate how molecular engineering can influence the charge transport in OFET devices.

In addition to the OFET devices; OPV devices were also fabricated and characterized. Recently, solution processable small molecules using D-A blocks have been used successfully for OPV devices.²⁶⁻²⁹ Bulk heterojunction OPV devices employed **BO-DPP-BTZ** as a donor with PCBM ([6,6]-Phenyl C71-butyric Acid Methyl Ester ([70]PCBM) as the acceptor in a 1:1 by wt. ratio were fabricated. The device structure was ITO/PEDOT:PSS/BHJ active layer/Al, and the active area was 0.09 cm². The active layer was spin coated from either a chloroform or chloroform: diiodooctane (1vol % DIO) solution and had a thickness around 80-100 nm. Bilayer devices were also

fabricated by evaporating a layer of C60 on top of an underlying film of **BO-DPP-BTZ** spin coated from chloroform; the device structure was: ITO/PEDOT:PSS/**BO-DPP-BTZ** (20 nm)/C60 (40 nm)/BPhen (6 nm) /Al, where bathophenanthroline (BPhen) was employed as an exciton blocking layer at the cathode contact. The current density-voltage (J-V) responses and the Incident Photon-to-collected-electron Conversion Efficiency (IPCE) spectra of the devices are shown in Figure 4. The key performance characteristics of **BO-DPP-BTZ**: [70] PCBM_BHJ and **BO-DPP-BTZ**/C60 bilayer OPV devices are summarized in Table 1.

Table 1. **BO-DPP-BTZ**: [70] PCBM BHJ OPV device parameters and **BO-DPP-BTZ**/C60 bilayer OPV device parameters

Devices	BHJ	BHJ with DIO	Bilayer
J_{sc} [mA/cm ²]	-1.20	-2.40	-1.70
V_{oc} [Volts]	0.81	0.78	0.69
FF	0.26	0.48	0.41
PCE [%]	0.26	0.89	0.50

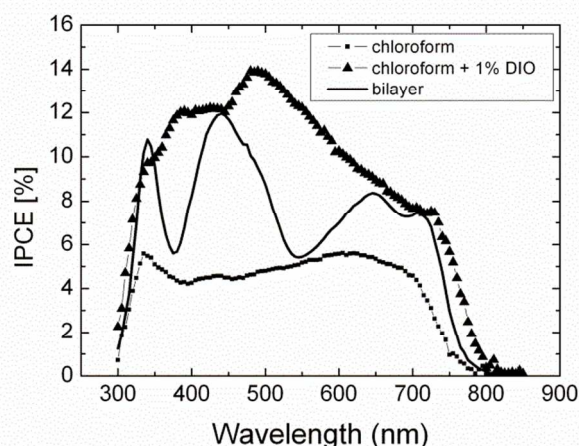
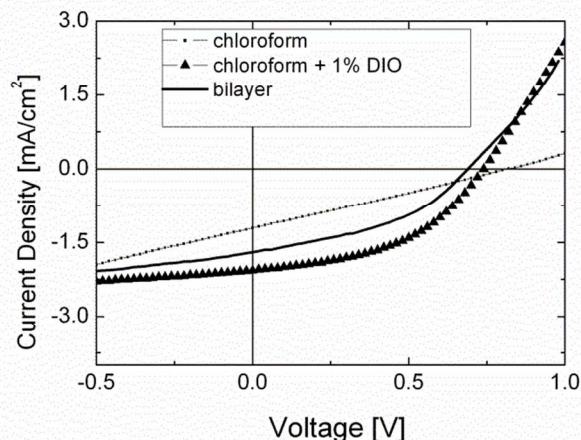


Fig. 4 Current density-voltage curves of the **BO-DPP-BTZ**: [70] PCBM(1:1) BHJ (upper) and the **BO-DPP-BTZ**/C60 bilayer OPV cells under dark and simulated AM1.5 conditions and the IPCE spectra (lower).

BHJ devices fabricated from the chloroform-only solution show the lowest performance with power conversion efficiency (PCE) of 0.26 %; the short circuit current (J_{sc}) is -1.20 mA/cm², the open-circuit voltage (V_{oc}) is 0.81 V, and the fill factor (FF) is 0.26. When DIO is incorporated into the solution, the device performance improves: a PCE of 0.89 %, a J_{sc} of -2.40 mA/cm², a V_{oc} of 0.78 V, and a FF of 0.48. Comparing the devices made from chloroform and chloroform:DIO, the IPCE spectrum of the device made with DIO shows a greater contribution to photocurrent at longer wavelengths; a small shoulder can be seen around 730 nm. This is in good agreement with both the UV-vis spectrum of the neat **BO-DPP-BTZ** film and the UV-vis spectrum of the chloroform + DIO BHJ thin film (supporting information) and suggests that, within the blend, the **BO-DPP-BTZ** is closely packed with significant intermolecular interaction. The UV-vis spectrum of the BHJ film spin coated from only chloroform (supporting information) shows an absorption peak around 630 and a shoulder around 690 nm, and while red-shifted with respect to the UV-vis spectrum of **BO-DPP-BTZ** in solution, it is not as red shifted and does not have the sharp peaks seen in the spectrum of the neat thin film around 670 nm and 730 nm. This lack of absorption in the long wavelength region is the reason for the poor photoresponse seen in the IPCE spectrum at longer wavelengths (> 700 nm). The fact that the **BO-DPP-BTZ** in the blend spin coated from chloroform does not absorb as strongly in the red as the neat thin film suggests that fullerene acceptor disrupts the close packing and interaction between **BO-DPP-BTZ** molecules. These spectral characteristics along with the device performance lead us to believe that the chloroform processed blend is more intimately mixed while the chloroform:DIO film has greater phase segregation and likely a better transport network. The shape of the long wavelength region (650 nm-750 nm) of the IPCE spectrum of the chloroform device closely resembles the absorption spectrum of the film. These characteristics of the absorption spectrum suggest that the **BO-DPP-BTZ** is better ordered and closer packed in the chloroform:DIO film than in the chloroform film.

Atomic Force Microscopy (AFM) was used to examine the topography of the blend films (supporting information). The AFM image of the BHJ film spin coated from chloroform shows that the film is quite smooth and relatively featureless. The image from the BHJ film spin coated from chloroform + DIO shows a film with larger surface roughness, overall, and some crystalline-like features, which are believed to be **BO-DPP-BTZ**. Induced segregation and the resultant close packing of the **BO-DPP-BTZ** in the DIO-containing film is in agreement with the spectral characteristics seen in the UV-vis spectrum. A bilayer device structure was also investigated to evaluate the performance in comparison with BHJ devices. **BO-DPP-BTZ** based bilayer devices showed modest performance and the PCE value is in between that of the chloroform + DIO device and the chloroform-only device. A PCE of 0.50 %, J_{sc} of -1.70 mA/cm², a V_{oc} of 0.69 V, and a FF of 0.41 were measured for the bilayer devices. The positions of the peaks in the spectral response closely resemble the peak positions seen in the UV-vis absorption spectra of a neat film of **BO-DPP-BTZ**.

Conclusions

A small molecule (**BO-DPP-BTZ**) end capped with benzothiadiazole using thiophene flanked diethylpyrrolopyrrole (DPP) as a central conjugated fused aromatic building block has been designed and synthesized via Suzuki coupling. Incorporation of electron withdrawing benzothiadiazole groups at the end of DPP gives an A-D-A-D-A type structure. Due to the

strong donor-acceptor interactions and solid state ordering, this molecule exhibits a significant red shift when comparing solution to solid state absorbance. **BO-DPP-BTZ** exhibits a small band gap of 1.50 eV, as determined from solid state UV-vis measurement. **BO-DPP-BTZ** based OFET devices exhibited a highest hole mobility of 0.06 cm²/Vs with low hysteresis. This is one of the higher mobility values reported for a simple, solution-processable DPP-based small molecule. Upon using this material as a donor with [70]PCBM as the acceptor in BHJ organic solar cells, a maximum PCE of 0.9% has been measured. The application of **BO-DPP-BTZ** for both high mobility OFETs and moderate PCE OPVs makes it a suitable choice for organic electronics.

Acknowledgements: Authors acknowledge to the Visiting Investigatorship Programme (VIP) of the Agency for Science, Technology and Research (A*STAR), Republic of Singapore for financial support. S.M. thanks the Ministry of Education of Singapore for support via the AcRF Tier 1 grant.

Notes and references

^a Institute of Materials Research and Engineering (IMRE), Agency for Science, Technology, and Research (A*STAR), 3 Research Link, Singapore 117602; E-mail: sonarp@imre.a-star.edu.sg
^b Current Address, Shiv Nadar University, Greater Noida, India.
^c Department of Mechanical Engineering Faculty of Engineering National University of Singapore Block E2 #05-02, 9 Engineering Drive 1 Singapore 117576
^d Microelectronics Research Centre, The University of Texas at Austin, Austin, TX, 78758, USA; E-mail: ananth.dodabalapur@engr.utexas.edu

†Electronic Supplementary Information (ESI) available: Experimental details and NMR data of compounds 2, 4 and BO-DPP-BTZ. See DOI: 10.1039/b000000x/

- (a) L. Biniek, B. C. Schroeder, C. B. Nielsen, I. McCulloch, *J. Mater. Chem.* 2012, **22**, 14803; (b) C. B. Nielsen, M. Turbiez, I. McCulloch, *Adv. Mater.* 2013, **25**, 1859.
- (a) A. C. Rochat, L. Cassar and A. Iqbal, U. S. patent, 1986, 4,579,949; (b) B. Tieke, A. R. Rabindranath, K. Zhang and Y. Zhu, *Beilstein J. Org. Chem.*, 2010, **6**, 830.
- Y. Li, P. Sonar, L. Murphy, W. Hong, *Energ. Environ. Sci.* 2013, DOI DOI: 10.1039/C3EE00015J
- (a) S. Qu, H. Tian, *Chem. Commun.*, 2012, **48**, 3039; (b) Y. Lin, Y. Lia, X. Zhan, *Chem. Soc. Rev.* 2012, **41**, 4245.
- A. B. Tamayo, B. Walker, T. Q. Nguuyen, *J. Phys. Chem. C* 2008, **112**, 11545.
- M. Tantiwiwat, A. Tamayo, N. Luu, X. D. Dang, and T. Q. Nguyen, *J. Phys. Chem. C* 2008, **112**, 17402.
- P. Sonar, G. M. Ng, T. T. Lin, A. Dodabalapur, Z. K. Chen, *J. Mat. Chem.* 2010, **20**, 3626.
- B. Walker, A. B. Tamayo, X. D. Dang, P. Zalar, J. H. Seo, A. Garcia, M. Tantiwiwat, and T.-Q. Nguyen, *Adv. Funct. Mater.* 2009, **19**, 1.

- S. L. Suraru, U. Zschieschang, H. Klauk, F. Wurthner, *Chem. Comm.* 2011, **47**, 1767.
- K. A. Mazzio, M. J. Yuan, K. Okamoto, C. K. Luscombe, *ACS Appl. Mater. & Inter.*, 2011, **3**, 271.
- J. Mei, K. R. Graham, R. Stalder, S. P. Tiwari, H. Cheun, J. Shim, M. Yoshio, C. Nuckolls, B. Kippelen, R. K. Castellano, J. R. Reynolds, *Chem. Mater.* 2011, **23**, 2285.
- S. Losers, C. J. Bruns, H. Miyauchi, R. P. Ortiz, A. Facchetti, S. I. Stupp, T. J. Marks, *J. Am. Chem. Soc.* 2011, **133**, 8142.
- O. P. Lee, A. T. Yiu, P. M. Beaujuge, C. H. Woo, T. W. Holcombe, J. E. Millstone, J. D. Douglas, M. S. Chen, J. M. J. Frechet, *Adv. Mater.* 2011, **23**, 5359.
- Y. Lin, P. Cheng, Y. Li, X. Zhan, *Chem. Comm.* 2012, **48**, 4773.
- D. Sahu, C. H. Tsai, H. Y. Wei, K. C. Ho, F. C. Chang, C. W. Chu, *J. Mat. Chem.* 2012, **22**, 7945.
- P.-Luc T. Boudreault, J. W. Hennek, S. Loser, R. P. Ortiz, B. J. Eckstein, A. Facchetti, T. J. Marks, *Chem. Mater.*, 2012, **24**, 2929.
- (a) Y. Qiao, Y. Guo, C. Yu, F. Zhang, W. Xu, Y. Liu, D. Zhu, *J. Am. Chem. Soc.*, 2012, **134**, 4084; (b) H. Zhong, J. Smith, S. Rossbauer, A. J. P. White, T. D. Anthopoulos, M. Heeney, *Adv. Mater.*, 2012, **24**, 3205.
- J. M. Hancock, A. P. Gifford, Y. Zhu, Y. Lou and S. A. Jenekhe, *Chem. Mater.*, 2006, **18**, 4924.
- K. Pilgram, M. Zupan and R. Skiles, *J. Heterocycl. Chem.*, 1970, **7**, 6216. P.-Luc T. Boudreault, J. W. Hennek, S. Loser, R. P. Ortiz, B. J. Eckstein, A. Facchetti, T. J. Marks, *Chem. Mater.*, 2012, **24**, 2929.
- A. D. Becke, *J. Chem. Phys.*, 1993, **98**, 5648.
- J. Tomasi, B. Mennucci, and R. Cammi, *Chem. Rev.*, 2005, **105**, 2999.
- T. Yanai, D. Tew, and N. Handy, *Chem. Phys. Lett.*, 2004, **393**, 51.
- Gaussian 09, Revision A.1, M. J. Frisch, G. W. Trucks, H. B. Schlegel, G. E. Scuseria, M. A. Robb, J. R. Cheeseman, G. Scalmani, V. Barone, B. Mennucci, G. A. Petersson, H. Nakatsuji, M. Caricato, X. Li, H. P. Hratchian, A. F. Izmaylov, J. Bloino, G. Zheng, J. L. Sonnenberg, M. Hada, M. Ehara, K. Toyota, R. Fukuda, J. Hasegawa, M. Ishida, T. Nakajima, Y. Honda, O. Kitao, H. Nakai, T. Vreven, J. A. Montgomery, Jr., J. E. Peralta, F. Ogliaro, M. Bearpark, J. J. Heyd, E. Brothers, K. N. Kudin, V. N. Staroverov, R. Kobayashi, J. Normand, K. Raghavachari, A. Rendell, J. C. Burant, S. S. Iyengar, J. Tomasi, M. Cossi, N. Rega, J. M. Millam, M. Klene, J. E. Knox, J. B. Cross, V. Bakken, C. Adamo, J. Jaramillo, R. Gomperts, R. E. Stratmann, O. Yazyev, A. J. Austin, R. Cammi, C. Pomelli, J. W. Ochterski, R. L. Martin, K. Morokuma, V. G. Zakrzewski, G. A. Voth, P. Salvador, J. J. Dannenberg, S. Dapprich, A. D. Daniels, Ö. Farkas, J. B. Foresman, J. V. Ortiz, J. Cioslowski, and D. J. Fox, Gaussian, Inc., Wallingford CT, 2009.
- (a) J. Roncali, *Chem. Rev.*, 1992, **92**, 711; (b) J. Roncali, *Chem. Rev.*, 1997, **97**, 173.
- A. K. Palai, H. Cho, S. Cho, T. J. Shin, S. Jang, S. U. Park, S. Pyo, *Org. Elect.* 2013, **14**, 1396.
- Y. Yamashita, *Sci. Technol. Adv. Mater.*, 2009, **10**, 024313
- F. Linker, B. Heinrich, R. De Bettignies, P. Rannou, J. Pécaut, B. Grévin, A. Pron, B. Donnio, R. Demadrille, *J. Mat. Chem.* 2011, **21**, 5238-5247.
- Q. Shi, P. Cheng, Y. Li and X. Zhan, *Adv. Energy Mater.*, 2012, **2**, 63
- W. Shin, T. Yasuda, G. Watanabe, Y. S. Yang, C. Adachi, *Chem. Mat.* 2013, **25**, 2549
- B. Walker, J. Liu, C. Kim, G. C. Welch, J. K. Park, J. Lin, P. Zalar, C. M. Proctor, J. H. Seo, G. C. Bazan, T. Q. Nguyen, *Energy Environ. Sci.*, 2013, **6**, 952